ACS OMEGA

Article

Cite This: ACS Omega 2018, 3, 8067−8073

High Bending-Mode Sensitivity of Printed Piezoelectric Poly(vinylidenefluoride-*co*-trifluoroethylene) Sensors

Satu Rajala,[†] Martijn Schouten,[‡] Gijs Krijnen,[‡] and Sampo Tuukkanen*[,§]

[†]Nokia Technologies, Karaportti 4, FI-02610 Espoo, Finland

[‡]Robotics and Mechatronics Research Group, Faculty of Electrical Engineering, University of Twente, P.O. Box 217, 7500 AE Enschede, Netherlands

[§]BioMediTech Institute and Faculty of Biomedical Sciences and Engineering, Tampere University of Technology, P.O. Box 692, FI-33101 Tampere, Finland

ABSTRACT: Printable piezoelectric sensors were fabricated on a flexible polyethylene terephthalate (PET) substrate. Solution-processed piezoelectric poly(vinylidenefluoride-*co*-trifluoroethylene) ink was used as an active layer. Evaporated silver on PET was used as the bottom electrode and the painted silver glue as the top electrode. The sensors were poled using a high dc electric field from 25 to 65 MV m^{-1}, yielding piezoelectric normal direction sensitivities up to 25 pC N^{-1}. Bending-mode sensitivities showed values up to 200 nC N^{-1}, which is 4 orders of magnitude larger than the force sensitivity in the normal direction. The high bending-mode sensitivities suggest suitability for detecting small forces, such as single fiber bonds or cardiomyocyte cell-beating force.

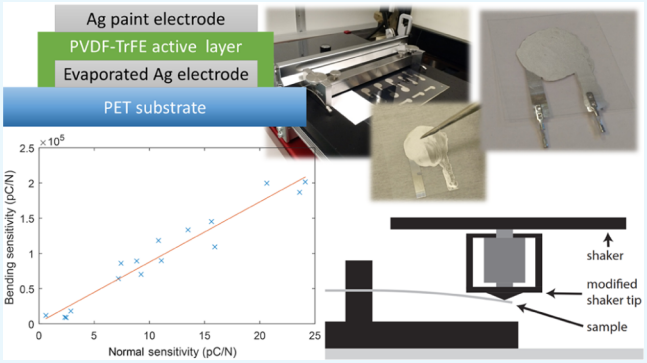

1. INTRODUCTION

Polyvinylidenefluoride (PVDF) is a piezoelectric viscoelastic, semicrystalline material that generates a charge when it is mechanically deformed. PVDF and its copolymers, especially with trifluoroethylene (TrFE), have become important piezoelectric materials for sensor applications.[1] There are several applications in the fields of mechanical (such as pressure, acceleration, vibration, and tactile sensors), acoustics, and infrared radiation sensors.[2] Other application areas include, for example, energy conversion and harvesting,[3,4] touch panels,[5] resistive switching devices,[6] and physiological measurement.[7] Recently, biological materials such as wood-based nanocellulose,[8] bacterial nanocellulose,[9] and chitosan[10] have been demonstrated as piezoelectric materials, but their piezoelectric response still remains weaker than PVDF and its copolymers.

Conventionally, piezoelectric PVDF films are manufactured by bringing the PVDF resin pellets into a sheet form with melt extrusion and stretching the sheet.[11] Different crystal phases exist in PVDF: the alpha phase is the most stable phase at room temperature, whereas the β phase shows the highest piezoelectric effect.[12,13] Stretching at a temperature below the melting point causes chain packaging of the molecules into parallel crystal planes (β phase).[11] These electric dipole moments are randomly oriented and result in zero net polarization.[12] In the poling stage, the stretched polymer is exposed to a high electric field to generate piezoelectric properties.[11] The poling procedure, in general, consists of applying an electric field for a certain period of time.[14] The molecular dipoles are oriented in the direction of the electric field, and an overall net polarization is obtained for the film.[12] The printable copolymer poly(vinylidenefluoride-*co*-trifluoroethylene) [P(VDF-TrFE)], which is prepared by copolymerization of TrFE and vinylidene, can be poled with a similar method.[15]

PVDF and P(VDF-TrFE) are both semicrystalline polymers: they are comprised of ordered regions of monomer units, crystallites, surrounded by amorphous chains.[15] The P(VDF-TrFE) polymer has some advantages when compared to PVDF: with P(VDF-TrFE), the β phase can be obtained directly by adding a copolymer, and only poling using electric field is necessary for piezoelectricity and no stretching is needed.[16,17] In addition, the crystallinity, remanent polarization, and temperature stability of P(VDF-TrFE) are higher than those of PVDF.[16]

Some methods to fabricate P(VDF-TrFE) sensors have been reported previously. Haque et al. developed inkjet-printed films using high-molecular-weight P(VDF-TrFE).[18] They used a modified waveform and a very low jetting frequency to accommodate the relaxation time of the polymeric ink during jetting. The films were characterized to investigate their morphology and crystallinity. Persano et al. fabricated and characterized pressure sensors that consist of sheets of electrospun fibres of P(VDF-TrFE).[19] Ducrot et al. studied the influence of processing parameters on P(VDF-TrFE)

Received: May 30, 2018
Accepted: July 11, 2018
Published: July 23, 2018

DOI: 10.1021/acsomega.8b01185
ACS Omega 2018, 3, 8067−8073

piezoelectric properties.[16] The influence of parameters, including poling field, poling time, and annealing duration, of spin-coated films were studied. The fabricated P(VDF-TrFE) thin films were used as integrated transducers in organic microelectromechanical systems resonators. Sharma et al. microfabricated and characterized P(VDF-TrFE)-based pressure sensors to be integrated with a catheter for intravascular measurements.[20] Lithographic-based fabrication process was used. Bhavanasi et al. used P(VDF-TrFE) for energy harvesting.[21] They reported the enhanced piezoelectric energy harvesting performance of the bilayer films of poled P(VDF-TrFE) and graphene oxide. Dodds et al. fabricated and characterized nanocomposite films based on P(VDF-TrFE) and zinc oxide (ZnO) nanoparticles.[22] ZnO particles were used to enhance the bulk film piezoelectricity. Khan et al. used an all screen-printing technique to fabricate P(VDF-TrFE) and P(VDF-TrFE)/multiwalled carbon nanotube pressure sensors.[23] Zirkl et al. demonstrated an allprinted matrix sensor array using P(VDF-TrFE) as the sensor ink.[24] Rendl et al. used a printable piezoelectric P(VDF-TrFE) film as an active layer in their sensors and conductive polymer (PEDOT:PSS) and carbon as electrode materials.[25,26]

In this study, piezoelectric sensors were fabricated from a printable P(VDF-TrFE) ink on a flexible plastic substrate. Our aim was to develop a low-cost and fast process for the fabrication of flexible piezoelectric sensors under ambient conditions. The sensors were subsequently poled with a high dc electric field, and their piezoelectric sensitivities in normal and bending modes were measured. An analytical model for a sensor operating in the bending mode was also derived here. Remarkably high bending-mode sensitivity observed here suggests that the sensors are suitable for very low dynamic force measurements in various applications such as a single fiber bond or a single living cell force response measurements.

2. MATERIALS AND METHODS

2.1. Piezoelectric Coefficients. The generated charge density in piezoelectric polymers is defined as

$$D = \frac{Q}{A} = d_{mn}X_n = d_{3n}X_n \quad (1)$$

where Q is the charge developed by the sensor, A is the conductive electrode area, d_{3n} is the piezoelectric coefficient for the axis of applied stress, and X_n is the stress applied in the relevant direction. For the electrical axis, m is, in our case, always 3 because the electrodes are at the top and bottom of the film. In the normal mode also, the mechanical axis n is 3. In the bending mode, the electrical signal is mainly due to bending or stretching in the lateral mode (length and width of the sensors, mechanical axes 1 and 2).

2.2. Fabrication of P(VDF-TrFE) Sensors. Commercial P(VDF-TrFE) ink (Solvene 250, casting formulation, Solvay, Belgium) with inherent piezo-, pyro-, and ferroelectric properties were applied in the sensor application.[27] This P(VDF-TrFE) ink had a VDF/TrFE molar ratio of 3:1. Table 1 lists the properties of the ink.

A transparent and flexible polyethylene terephthalate (PET) film (Melinex ST506) of thickness 125 μm was used as a substrate for the sensor. To provide a bottom electrode for the sensor, a 100 nm-thick layer of silver (Ag) was vacuum-evaporated (System Control Technologies, USA, with 880 Deposition Controller, Telemark, USA) on PET. A mechanical shadow mask made of PET was used to obtain the electrode pattern. The electrodes have a circular shape with a diameter of 20 mm with branching contact areas (see Figure 1a).

An automatic film applicator (ZAA 2300 Automatic Film Applicator, Zehntner, Switzerland) equipped with a coating

Table 1. Properties of the P(VDF-TrFE) Ink Given by the Manufacturer (Solvene 250, Casting Formulation, Solvay, Belgium)[27]

physical form	solution
melting temperature	142 °C
crystallization temperature	123 °C
Curie temperature	110 °C
glass transition temperature	−37 °C
density (liquid)	0.84 g cm^{-3}
density (film)	1.48 g cm^{-3}
boiling point	79 °C
viscosity	1500 cP
target thickness range	9−80 μm
drying temperature	100 °C
annealing temperature (max)	130 °C
d_{33}[a]	−22 pC N^{-1}
coercive field[a]	80 V μm^{-1}
poling field (min)	150 V μm^{-1}
poling field (max)	200 V μm^{-1}
remanent polarization (max)[a]	>6 μC cm^{-2}
breakdown voltage[a]	250 V μm^{-1}
ϵ_r (with 1 MHz)[a]	14

[a]Values obtained by poling at 200 V μm^{-1}, using a 25 μm-thick printed P(VDF-TrFE) layer.

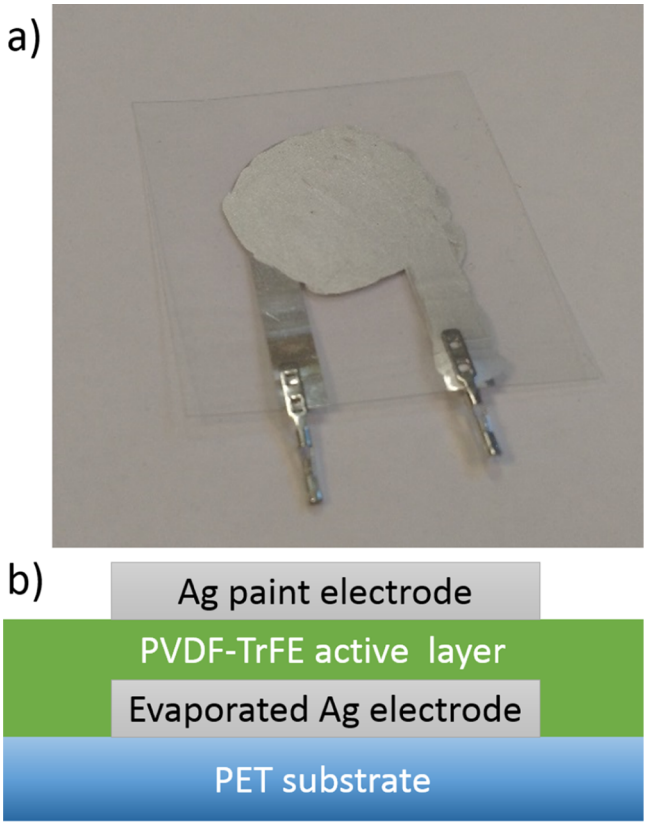

Figure 1. (a) Photograph of the sensor (diameter 20 mm) and (b) schematic cross-sectional view of the sensor. Note that the P(VDF-TrFE) layer and the PET substrate are transparent.

DOI: 10.1021/acsomega.8b01185
ACS Omega 2018, 3, 8067−8073

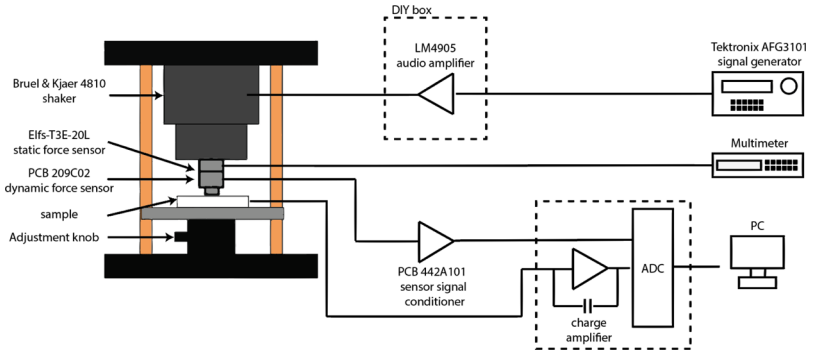

Figure 2. Shaker setup used in piezoelectric measurements.

tool (UA 3000-220 Universal Film Applicator, MTV Messtechnik, Germany) was used for deposition of a certain thickness of the P(VDF-TrFE) ink on the PET substrate and on the bottom electrode. To make the P(VDF-TrFE) ink viscosity suitable for the film applicator, the ink was diluted with methyl ethyl ketone (MEK) in a ratio of 1:2 [P(VDF-TrFE):MEK] by weight. MEK was selected as the dilution solvent as it is the same solvent used in the original P(VDF-TrFE) ink formulation. The universal applicator was set to a thickness of 350 μm, which defines the wet thickness of the ink film. For each sensor, two coated ink layers were used to improve the sensing layer quality. The coated P(VDF-TrFE) layer with the underlying evaporated silver electrode was then baked at 120 °C for 3 h in an oven. The P(VDF-TrFE) ink layer was deposited on an area slightly larger than the round bottom electrode area, and after deposition and baking, the PET substrate was cut smaller so that the ink film fully covers the final sensor substrate, as can be seen from Figure 1b.

A silver paint (conductive silver L100 from Kemo Electronic, 1-ethoxypropan-2-ol, and acetone ethyl acetate were used as solvents) layer was painted on top of the ink with a brush and used as the top electrode. Finally, crimp connectors (Nicomatic CrimpFlex, Nicomatic, France) were used to provide the electrical connection for the measurements. Figure 1a shows a photograph of the fabricated sensor, and Figure 1b shows the schematic cross-sectional structure of the sensor.

The assembled sensors were poled at room temperature using a high dc voltage source equipment (Spellman SL50-10, USA). This step was done to align the dipoles with the electric field and, thus, to cause a significant piezoelectric response.[16] The sensors were poled with field strengths varying from 25 to 55 MV m^{-1}. Each sensor was kept at this voltage for 1 h. A current limit of 100 μA was used in the voltage source. For the poling, the samples were connected using a custom-made 3D printed sample holder, which allows multiple sensors to be polarized at the same time.

To estimate the thickness of the P(VDF-TrFE) layer, the thickness d was calculated from the sensor capacitance ($d = \epsilon_0\epsilon_r A/C$), under the assumption that the relative permittivity $\epsilon_r = 14$ and $A = \pi r^2$. The capacitances of the sensors were measured with a multimeter. The capacitance offset caused by the measurement wires and the multimeter itself was subtracted from the measurement result. The applied poling field was then calculated using the thickness that was calculated from the capacitance. In comparison, the sensor thicknesses were also measured using a precision micrometer screw (Insize 3101-25A, resolution 1 μm) from seven different positions on the sensor area (see Figure 3a). However, because the bar-coated P(VDF-TrFE) layers were rather uneven, it was decided to use the effective thickness calculated from the measured capacitance for determining the poling field.

2.3. Normal Mode Sensitivity. The piezoelectric sensitivity was measured with a shaker generating a dynamic excitation force. The Brüel and Kjaer Mini-Shaker Type 4810 was used in the measurements. A sinusoidal input for the shaker was provided with a Tektronix AFG3101 function generator. A pretension, which produces a static force, is needed to keep the sample in place and prevent piston jumping during the measurement. A commercial, high-sensitivity dynamic force sensor (model number 209C02, PCB Piezotronics, USA) and a load cell (model number ELFS-T3E-20L, Measurement Specialties Inc., USA) were used as the reference sensors for measuring the applied dynamic and static forces. The dynamic force sensor was connected to a sensor signal conditioner (model 442B06, PCB Piezotronics, USA). Figure 2 presents the schematic overview of the setup.

To measure the piezoelectric d_{33} coefficient, the sample was placed horizontally on a steel table, as shown in Figure 3a. Bare

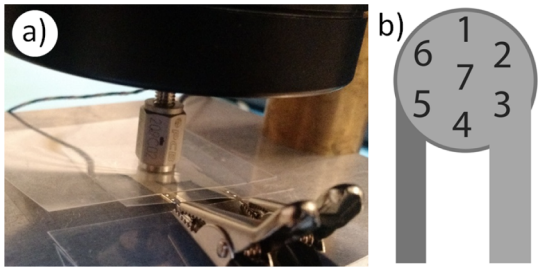

Figure 3. (a) Setup for the normal direction force piezoelectric sensitivity measurement. (b) Positions on a sensor used for sensitivity and thickness measurements.

PET films were placed on both sides of the sensor to prevent direct electric contact with the bottom plate and the shaker head. A static force of approximately 3 N between the sensor and the shaker's piston was adjusted to keep the sensor sample in place during the sinusoidal dynamic excitation force of 1.3 N at 2 Hz. Measurements were performed on seven different positions on the sample (Figure 3b) to reduce the influence of the surface roughness of the samples and the fact that the sample is placed under the shaker manually.

The charge generated by the sample as a result of the excitation force was measured with a custom-made combination of a charge amplifier and a 16-bit AD-converter. The AD-converter also had additional channels for sampling the voltage

DOI: 10.1021/acsomega.8b01185
ACS Omega 2018, 3, 8067−8073

signals from the reference sensors. In the measurements, a sampling rate of 1 kHz was used.

The dynamic force sensor and the charge amplifier signals were filtered using fast Fourier transform to remove the 50 Hz noise and baseline drift, so that only the 2 Hz signal component remained. The sensitivity is defined here as the charge generated by the sensor divided by the dynamic force used to excite the sensor. Because the excitation was sinusoidal, the calculation was done simply by dividing the amplitudes of the respective filtered sinusoidal signals.

2.4. Bending-Mode Sensitivity. To study the bending-mode sensitivity, the charge generated by the sensor was measured when it was bent. The stress when bending the sensor can be calculated using standard beam equations.[28] The stress in the P(VDF-TrFE) layer is then

$$\sigma_1 = E_p \varepsilon_1 = -6\frac{1}{wh}\frac{L-x}{h}\frac{E_p}{E_{PET}}F \quad (2)$$

where ε_1 is the strain, L is the length of the cantilever, x is the distance from the location where the cantilever is fixed, F is the applied force, E_p is the Young's modulus of P(VDF-TrFE), E_{PET} is the Young's modulus of PET, w is the width of the PET substrate, and h is the thickness of the PET sheet (see Figure 4). The charge in the P(VDF-TrFE) layer generated by this

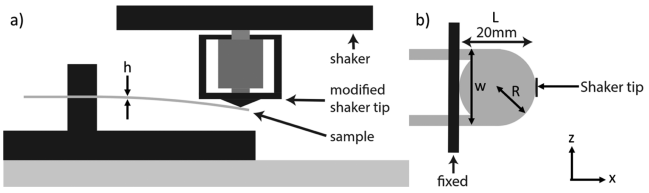

Figure 4. Schematic view of (a) the bending measurement setup and (b) sample assembly.

stress can be obtained by combining Gauss' law[29] with the relations for describing the piezoelectric material[30]

$$q = \oint D \, dS_e = \oint \sigma_1 d_{31} \, dS_e \quad (3)$$

where D is the electric displacement field, S_e is the surface of the electrode, and d_{31} (or d_{32}) is the lateral piezoelectric coefficient mostly relevant to the bending-mode sensor. However, there is also a slight contribution from the coefficient d_{33} to the bending-mode sensitivity, but it is here assumed to be remarkably smaller than that of d_{31}. For a rectangular PET substrate with a circular electrode, this integral evaluates to form

$$q = \int_{-R}^{R}\int_{R-\sqrt{R^2-z^2}}^{R+\sqrt{R^2-z^2}} -6\frac{d_{31}F(L-x)E_p}{wh^2E_{PET}}dx\,dz = -\frac{6\pi R^2(L-R)}{wh^2}\frac{E_p}{E_{PET}}d_{31}F \quad (4)$$

where R is the radius of the circular electrode and z is the distance from the neutral axis. The setup used in bending measurements is illustrated schematically in Figure 4, and the sample holder used is shown in Figure 5.

The bending-mode sensitivity for each sample was measured using different frequencies (1, 2, and 5 Hz) and different input amplitudes applied to the shaker (400, 500, and 600 mV). These input amplitudes resulted in physical z-direction

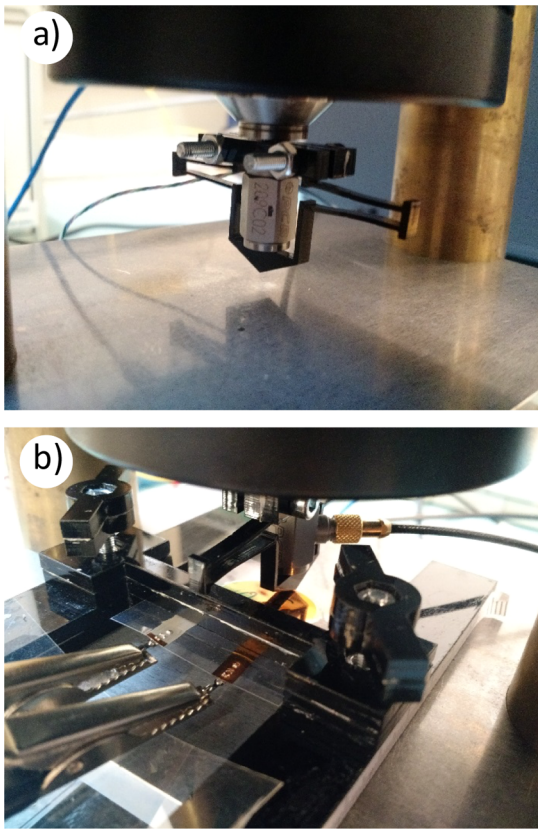

Figure 5. Photographs of the bending measurement setup. (a) A modified shaker head and (b) a sample assembled into the bending measurement holder.

movement amplitudes of about 0.8−1.2 mm. In total, all sensors were measured nine times.

3. RESULTS AND DISCUSSION

3.1. Yield and Thickness. The batch of fabricated 40 samples yielded 16 functional sensors. Several reasons were identified for a relatively large amount of nonfunctional samples. First, the deposition of the P(VDF-TrFE) layers under ambient conditions may lower the yield, presumably due to the appearance of dust particles on the substrate. This causes air gaps inside the sensing layer and decreases the dielectric strength in these locations because of the lower breakdown field of the air in comparison to P(VDF-TrFE). Figure 6 shows the number of survived and broken samples as a function of the poling field. Nine samples broke during the poling.

Further, eight samples showed a low resistance (<100 Ω) already before poling, indicating a short circuit through the P(VDF-TrFE) layer. This connection was removed before poling by connection a charged capacitor to the sensor. It is expected that a capacitor provides a large current density at the location of the short circuit, which evaporates the silver ink at this point, removing the connection between top and bottom electrodes. However, this treatment by a current pulse may increase the uncertainty on these samples.

The average capacitance of the sensors was (4.2 ± 1.2) nF. This corresponds to an average thickness of (9.2 ± 2.8) μm, under the assumption ϵ_r = 14. This permittivity value was given by the ink manufacturer and it was considered as a good estimate, but the real value may still be slightly different. It has

DOI: 10.1021/acsomega.8b01185
ACS Omega 2018, 3, 8067−8073

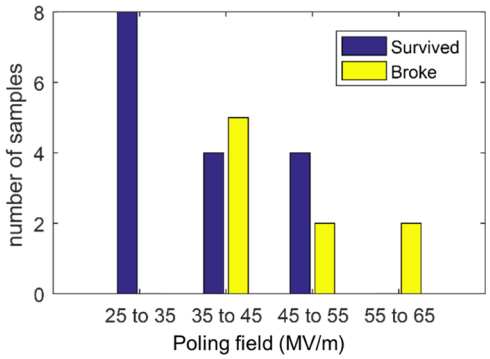

Figure 6. Number of samples that broke down at different poling fields.

to be noticed that the wet thickness of the deposited film was much thicker, but due to the low solid content of the ink, the final film thickness was relatively small. The average P(VDF-TrFE) layer thickness based on the precision micrometer screw measurement for all sensors was (6.7 ± 2.8) μm, which is slightly smaller than the average value calculated from the capacitance, most likely due to the unevenness of the bar-coated films.

To determine the poling field to polarize the samples, there are three parameters that have to be considered: these are the poling voltage, the poling time, and the thickness of the P(VDF-TrFE) layer. To accurately control these parameters, the poling voltage was measured with a multimeter, the poling time was measured with a timer, and the thickness of the samples was estimated using the measured capacitance data.

Ducrot et al. have studied the influence of poling conditions on the piezoelectric response of P(VDF-TrFE).[16] They reported the necessary electric field of about 100 MV m^{-1} under room-temperature conditions, whereas the field used in this study varied between 25 and 65 MV m^{-1}. Ducrot et al. also reported that the value of the electric field is more important than the poling time in determining the effectiveness of the poling process of P(VDF-TrFE): the duration of only 5 min at 100 V μm^{-1} is sufficient to reach the maximum level of remanent polarization and a longer poling does not bring any advantages.[16] Here, the sensors were polarized for 1 h, as the poling field used was lower than the value recommended. The lower poling field was used to improve the yield as the larger poling field increased the number of sensor samples that broke down. In addition, a few minutes of annealing is recommended to achieve the best piezoelectric property of P(VDF-TrFE).[16] Here, we did not use a separate annealing step after the baking of the coated P(VDF-TrFE) film, but the baking temperature we used corresponds to the recommended annealing temperature.

Generally, poling is carried out in a temperature-controlled oil bath.[17] However, we have performed the poling in ambient air, which may decrease the breakdown voltage of the sensors. Another reason for the decreased breakdown voltage is the appearance of small air bubbles inside the P(VDF-TrFE) films. Especially, as the samples were coated twice to improve the layer quality, there may have been pinholes in one of the layers that is covered by the other, causing a larger field at that location. Also, the dust particles deposited from the ambient air causes air gaps into the sensing layer, decreasing the breakdown field.

3.2. Normal Force Sensitivity. Figure 7 shows the measured normal-mode sensitivities as a function of the poling

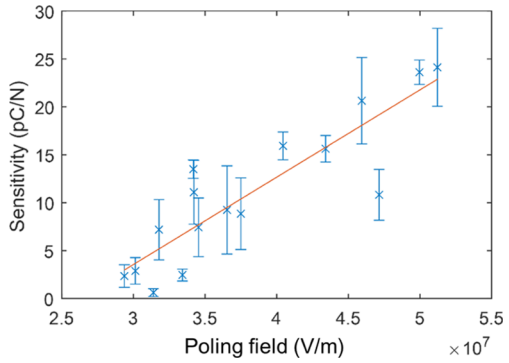

Figure 7. Measured normal-force sensitivity as a function of the poling field, which is derived from the capacitance under the assumption that ϵ_r = 14.

field. Error bars for normal-mode sensitivity, measured from seven locations from each sensor, are relatively large for some samples, which is most likely due to nonhomogeneity of the P(VDF-TrFE) film.

Concerning the yield of functional samples, the sensors with the normal-force sensitivity of 16.1 ± 6.1 pC N^{-1} had a yield of about 37% and 5.9 ± 4.6 pC N^{-1} had a yield of 78%. The higher poling field produced higher sensor sensitivity values, but also increased the amount of sensors that broke down during the poling step. Depending on the aim of future studies, a compromise between the yield and piezoelectric response should be made.

The normal-force sensitivity measured in this study is closely related to the piezoelectric d_{33} coefficient. The d_{33} coefficient, also called the longitudinal coefficient, describes the electrical polarization generated in the same direction as the stress is applied.[31] The d_{33} coefficient given for the P(VDF-TrFE) ink by the manufacturer is 22 pC N^{-1} (25 μm thick film with printed silver electrodes, poling at 200 V μm^{-1}).[27] The highest piezoelectric normal sensitivity values obtained in this study were close to 25 pC N^{-1}. However, the maximum sensitivity of the samples may not have been reached as a lower poling voltage than recommended was used.[13] As can be seen from Figure 7, the saturation of the sensor sensitivity was not reached here, and this may indicate that the poling was not complete. With higher poling voltages, the saturation of sensitivity could be achieved. More complete saturation could be achieved by using ac poling instead of dc poling. The high d_{33} coefficient may be also partly explained by the bending contribution: the compressibility of both the PET substrate and the PET protection sheets may cause bending forces that increase the measured normal-force sensitivity.

3.3. Bending-Force Sensitivity. Figure 8 shows the measured bending-mode sensitivities as a function of the poling field.

The measured maximum bending-mode sensitivity value (around 200 nC N^{-1}) corresponds to the d_{31} coefficient of about 6 pC N^{-1} (calculated from eq 4). For Young's modulus E_p, the literature[31] value 2.05 was used in the calculation of d_{31}, whereas for E_{PET}, we used a value of 3.6 GPa provided by the manufacturer of the PET film. For the P(VDF-TrFE) ink, the d_{31} coefficient is not given by the manufacturer. However, the d_{31} range of 6−12 pC N^{-1} has been reported for P(VDF-

DOI: 10.1021/acsomega.8b01185
ACS Omega 2018, 3, 8067−8073

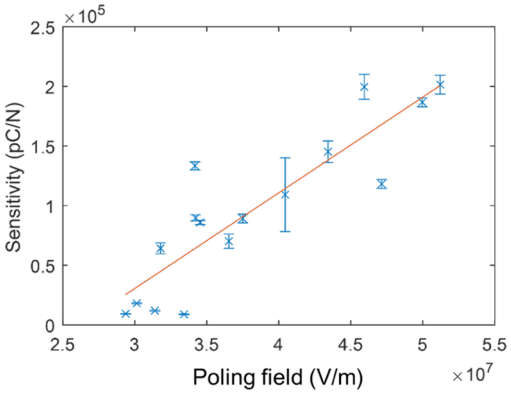

Figure 8. Measured bending-mode sensitivity as a function of the poling field, which is derived from the capacitance under the assumption that $\epsilon_r = 14$.

TrFE),[31] and the value obtained in this study is close to the minimum of that range.

The bending-mode sensitivities were further compared with normal-mode sensitivities. Figure 9 shows the bending-mode

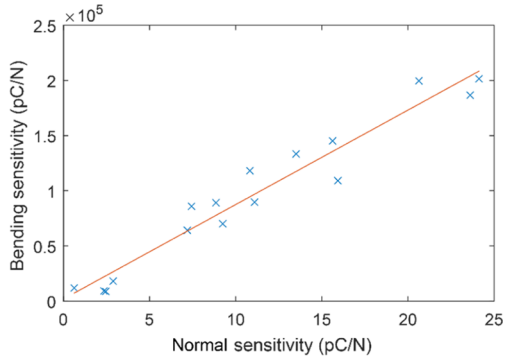

Figure 9. Bending-mode sensitivity against the normal-mode sensitivity.

sensitivity results as a function of the normal-mode force sensitivity results. As can be seen, the response is linear: the sensor having a higher normal-mode sensitivity also has a higher bending-mode sensitivity.

The average bending sensitivity obtained for the sensors polarized with a field between 35−65 MV m^{-1} was found to be 140 ± 50 nC N^{-1}. However, the dependency between the bending and normal force modes is rather linear, suggesting that high normal force sensitivity also indicates a high bending force sensitivity value.

A similar method based on bending force measurements has been previously used by Saketi et al. to measure strength in paper fiber ponds.[32] They developed a microforce PVDF sensor that operates in a cantilever-like bending mode. In the case of the printed sensor, the substrate material mostly defines the Young's modulus of the sensor structure in comparison to use of the self-standing PVDF film with thin electrodes. As an additional advantage of the printed sensors, the sensor operation range can be fine-tuned by selecting the desired substrate material giving certain mechanical properties. Both in the bending and normal force sensors, the mechanical properties of the selected substrate can be used to modify the sensor operation range.

4. CONCLUSIONS

The aim of this study was to develop a low-cost and fast process for fabrication of flexible piezoelectric sensors under ambient conditions. In addition to the sensor fabrication process, poling was also done under ambient conditions. One should notice, however, that the fabrication of the bottom electrode was done here by the vacuum evaporation process. This was the only step requiring vacuum processing, but instead one could use prepatterned or fully metallized and wet-etched bottom electrodes, enabling sensor structure processing under ambient conditions. This manufacturing approach is generally considered as the roll-to-roll compatible fabrication technique.

To conclude, the solution-processed piezoelectric sensors were fabricated using P(VDF-TrFE) ink as an active layer. The fabricated sensors were characterized in the normal and bending mode setups. Normal-mode sensitivities showed values up to 25 pC N^{-1}, whereas bending-mode sensitivities showed remarkably high values up to 200 nC N^{-1}. The cantilever-type bending-mode measurement demonstrated in this study can be utilized for a low force detection required, for example, in single fiber or living cell level measurements.

AUTHOR INFORMATION

Corresponding Author

*E-mail: sampo.tuukkanen@tut.fi (S.T.).

ORCID

Sampo Tuukkanen: 0000-0002-4090-7278

Notes

The authors declare no competing financial interest.

REFERENCES

(1) Wang, H.; Zhang, Q. M.; Cross, L. E.; Sykes, A. O. Piezoelectric, Dielectric, and Elastic Properties of Poly(vinylidene Fluoride/trifluoroethylene). *J. Appl. Phys.* **1993**, *74*, 3394−3398.

(2) Harsányi, G. Polymer Films in Sensor Applications: A Review of Present Uses and Future Possibilities. *Sens. Rev.* **2000**, *20*, 98−105.

(3) Lang, S. B.; Muensit, S. Review of Some Lesser-Known Applications of Piezoelectric and Pyroelectric Polymers. *Appl. Phys. A: Mater. Sci. Process.* **2006**, *85*, 125−134.

(4) Porhonen, J.; Rajala, S.; Lehtimaki, S.; Tuukkanen, S. Flexible Piezoelectric Energy Harvesting Circuit With Printable Supercapacitor and Diodes. *IEEE Trans. Electron Devices* **2014**, *61*, 3303−3308.

(5) Vuorinen, T.; Zakrzewski, M.; Rajala, S.; Lupo, D.; Vanhala, J.; Palovuori, K.; Tuukkanen, S. Printable, Transparent, and Flexible Touch Panels Working in Sunlight and Moist Environments. *Adv. Funct. Mater.* **2014**, *24*, 6340−6347.

(6) Rajan, K.; Bocchini, S.; Chiappone, A.; Roppolo, I.; Perrone, D.; Bejtka, K.; Ricciardi, C.; Pirri, C. F.; Chiolerio, A. Spin-Coated Silver Nanocomposite Resistive Switching Devices. *Microelectron. Eng.* **2017**, *168*, 27−31.

(7) Rajala, S.; Lekkala, J. Film-Type Sensor Materials PVDF and EMFi in Measurement of Cardiorespiratory Signals—A Review. *IEEE Sens. J.* **2012**, *12*, 439−446.

(8) Rajala, S.; Siponkoski, T.; Sarlin, E.; Mettänen, M.; Vuoriluoto, M.; Pammo, A.; Juuti, J.; Rojas, O. J.; Franssila, S.; Tuukkanen, S. Cellulose Nanofibril Film as a Piezoelectric Sensor Material. *ACS Appl. Mater. Interfaces* **2016**, *8*, 15607−15614.

(9) Mangayil, R.; Rajala, S.; Pammo, A.; Sarlin, E.; Luo, J.; Santala, V.; Karp, M.; Tuukkanen, S. Engineering and Characterization of Bacterial Nanocellulose Films as Low Cost and Flexible Sensor Material. *ACS Appl. Mater. Interfaces* **2017**, *9*, 19048−19056.

DOI: 10.1021/acsomega.8b01185
ACS Omega 2018, 3, 8067−8073

(10) Hänninen, A.; Rajala, S.; Salpavaara, T.; Kellomäki, M.; Tuukkanen, S. Piezoelectric Sensitivity of a Layered Film of Chitosan and Cellulose Nanocrystals. *Procedia Eng.* **2016**, *168*, 1176−1179.
(11) Measurement Specialties Inc. Piezo film sensors. Technical Manual http://www.meas-spec.com (accessed Feb 14, 2015).
(12) Eberle, G.; Schmidt, H.; Eisenmenger, W. Piezoelectric Polymer Electrets. *IEEE Trans. Dielectr. Electr. Insul.* **1996**, *3*, 624−646.
(13) Chiolerio, A.; Lombardi, M.; Guerriero, A.; Canavese, G.; Stassi, S.; Gazia, R.; Cauda, V.; Manfredi, D.; Chiodoni, A.; Verna, A.; Cocuzza, M.; Montanaro, L.; Pirri, C. F. Effect of the Fabrication Method on the Functional Properties of BaTiO3: PVDF Nanocomposites. *J. Mater. Sci.* **2013**, *48*, 6943−6951.
(14) Furukawa, T. Piezoelectricity and Pyroelectricity in Polymers. *IEEE Trans. Electr. Insul.* **1989**, *24*, 375−394.
(15) Zhang, Q. M.; Bharti, V.; Kavarnos, G. Poly (vinylidene fluoride)(PVDF) and its copolymers. In *Encyclopedia of Smart Materials*; Schwartz, M., Ed.; John Wiley & Sons, Inc.: Hoboken, NJ, USA, 2002.
(16) Ducrot, P.-H.; Dufour, I.; Ayela, C. Optimization Of PVDF-TrFE Processing Conditions For The Fabrication Of Organic MEMS Resonators. *Sci. Rep.* **2016**, *6*, 19426.
(17) Chan, H. L. W.; Zhao, Z.; Kwok, K. W.; Choy, C. L.; Alquié, C.; Boué, C.; Lewiner, J. Polarization of Thick Polyvinylidene Fluoride/trifluoroethylene Copolymer Films. *J. Appl. Phys.* **1996**, *80*, 3982−3991.
(18) Haque, R. I.; Vié, R.; Germainy, M.; Valbin, L.; Benaben, P.; Boddaert, X. Inkjet Printing of High Molecular Weight PVDF-TrFE for Flexible Electronics. *Flexible Printed Electron.* **2016**, *1*, 015001.
(19) Persano, L.; Dagdeviren, C.; Su, Y.; Zhang, Y.; Girardo, S.; Pisignano, D.; Huang, Y.; Rogers, J. A. High Performance Piezoelectric Devices Based on Aligned Arrays of Nanofibers of Poly(vinylidenefluoride-Co-Trifluoroethylene). *Nat. Commun.* **2013**, *4*, 1633.
(20) Sharma, T.; Je, S.-S.; Gill, B.; Zhang, J. X. J. Patterning Piezoelectric Thin Film PVDF−TrFE Based Pressure Sensor for Catheter Application. *Sens. Actuators, A* **2012**, *177*, 87−92.
(21) Bhavanasi, V.; Kumar, V.; Parida, K.; Wang, J.; Lee, P. S. Enhanced Piezoelectric Energy Harvesting Performance of Flexible PVDF-TrFE Bilayer Films with Graphene Oxide. *ACS Appl. Mater. Interfaces* **2016**, *8*, 521−529.
(22) Dodds, J. S.; Meyers, F. N.; Loh, K. J. Piezoelectric Characterization of PVDF-TrFE Thin Films Enhanced with ZnO Nanoparticles. *IEEE Sens. J.* **2012**, *12*, 1889−1890.
(23) Khan, S.; Dang, W.; Lorenzelli, L.; Dahiya, R. Flexible Pressure Sensors Based on Screen-Printed P(VDF-TrFE) and P(VDF-TrFE)/MWCNTs. *IEEE Trans. Semicond. Manuf.* **2015**, *28*, 486−493.
(24) Zirkl, M.; Sawatdee, A.; Helbig, U.; Krause, M.; Scheipl, G.; Kraker, E.; Ersman, P. A.; Nilsson, D.; Platt, D.; Bodö, P.; Bauer, S.; Domann, G.; Stadlober, B. An All-Printed Ferroelectric Active Matrix Sensor Network Based on Only Five Functional Materials Forming a Touchless Control Interface. *Adv. Mater.* **2011**, *23*, 2069−2074.
(25) Rendl, C.; Greindl, P.; Haller, M.; Zirkl, M.; Stadlober, B.; Hartmann, P.. PyzoFlex: Printed Piezoelectric Pressure Sensing Foil. *Proceedings of the 25th Annual ACM Symposium on User Interface Software and Technology—UIST '12*, 2012.
(26) Rendl, C.; Haller, M.; Izadi, S.; Kim, D.; Fanello, S.; Parzer, P.; Rhemann, C.; Taylor, J.; Zirkl, M.; Scheipl, G.; Rothländer, T. FlexSense: A Transparent Self-Sensing Deformable Surface. *Proceedings of the 25th Annual ACM Symposium on User Interface Software and Technology—UIST '14*, 2014.
(27) Solvay. *Solvene® 250 EAP Inks*, Technical Data Sheet, 2015.
(28) Webster, J. G.; Eren, H. *Measurement, Instrumentation and Sensors Handbook*; CRC Press, 1999.
(29) Griffiths, D. J. *Introduction to Electrodynamics*; Prentice Hall, 1999.
(30) Damjanovic, D. Ferroelectric, Dielectric and Piezoelectric Properties of Ferroelectric Thin Films and Ceramics. *Rep. Prog. Phys.* **1998**, *61*, 1267−1324.
(31) Ramadan, K. S.; Sameoto, D.; Evoy, S. A Review of Piezoelectric Polymers as Functional Materials for Electromechanical Transducers. *Smart Mater. Struct.* **2014**, *23*, 033001.
(32) Saketi, P.; Latifi, S. K.; Hirvonen, J.; Rajala, S.; Vehkaoja, A.; Salpavaara, T.; Lekkala, J.; Kallio, P. PVDF Microforce Sensor for the Measurement of Z-Directional Strength in Paper Fiber Bonds. *Sens. Actuators, A* **2015**, *222*, 194−203.

DOI: 10.1021/acsomega.8b01185
ACS Omega 2018, 3, 8067−8073